Atmospheric CO_2 during the Late Miocene Cooling

Thomas Tanner[1], Iván Hernández Almeida[1], Anna Joy Drury[2], José Guitián[1] and Heather Stoll[1]

[1]Geological Institute, ETH Zurich, Switzerland
[2]Department of Earth Science, University College London, UK

corresponding author: thomas.tanner@erdw.ethz.ch

from: "Decreasing atmospheric CO2 during the Late Miocene Cooling" - Tanner et al. *in review* in Paleoceanography and Paleoclimatology – The Miocene: The Future of the Past

Late Miocene Cooling

Climatic Background

- Moderate CO_2 levels
- Synchronous cooling in both hemispheres
- Sea-surface cooling of up to 6°C

hints to **CO_2 decrease**

Ecological Background

- Expansion of C_4 grasslands
- "vital effects" arise in coccolithophores

hints to **CO_2 decrease**

…but the proxy record is scarce for pCO_2 during the Late Miocene…

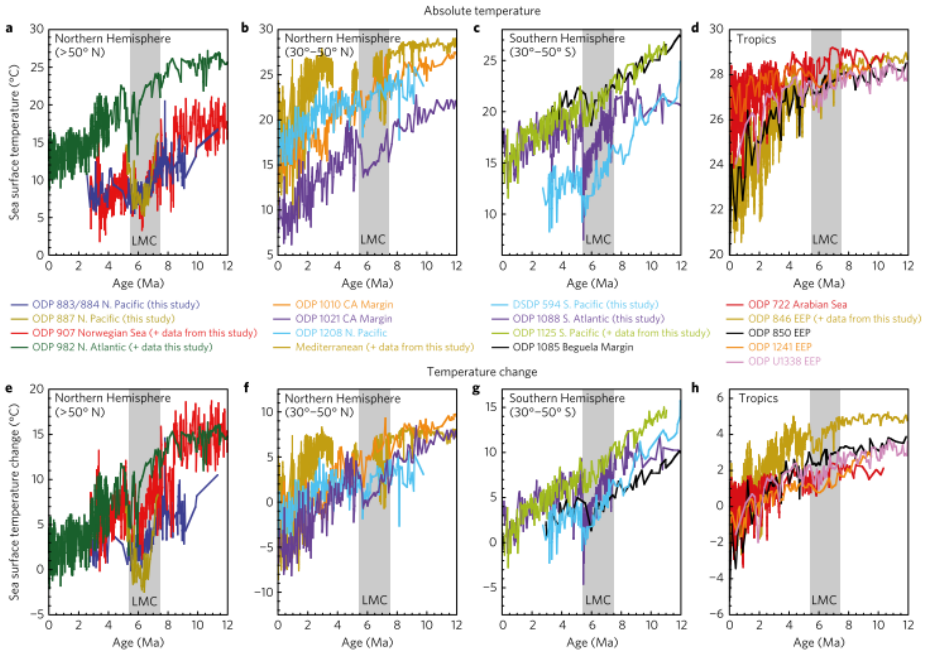

Figure 2 | Temperature evolution over the past 12 Myr for the sites in Fig. 1. a–d, Alkenone temperature records generated in this study or as previously published; all datasets use the calibration of ref. 23. **e–h**, SST changes as differences relative to the modern mean annual sea surface temperature at the site. Data are binned by latitude: Northern Hemisphere (>50° N); Northern Hemisphere (30°–50° N); Southern Hemisphere (30°–50° S); and Tropics. Grey highlighted interval is late Miocene cooling (LMC) common to all sites. Site information and citations for all datasets are available in Supplementary Table 1; see Methods for SST backtracking procedure.

Herbert et al. 2016

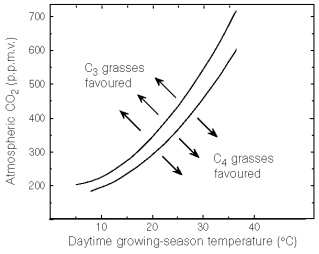

Cerling et al. 1997

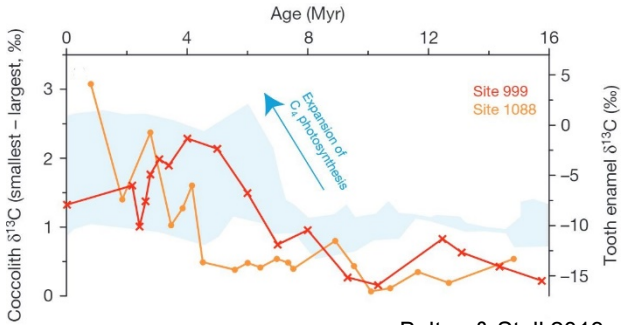

Bolton & Stoll 2013

Alkenone bases pCO_2 proxy

- Isotopic fractionation between DIC and carbon fixed during photosynthesis

$$\varepsilon_p = \left(\frac{\delta^{13}C_{[CO_2]_{aq}} + 1000}{\delta^{13}C_{org} + 1000} \right) * 1000$$

- Various factors influence ε_p

$$\varepsilon_p = \varepsilon_t + (\varepsilon_f - \varepsilon_t)\left(1 - \frac{\mu}{[CO_2]_{aq}} \frac{V}{S}\right)$$

Problem

growth rate (μ) cannot be measured in the sedimentary record

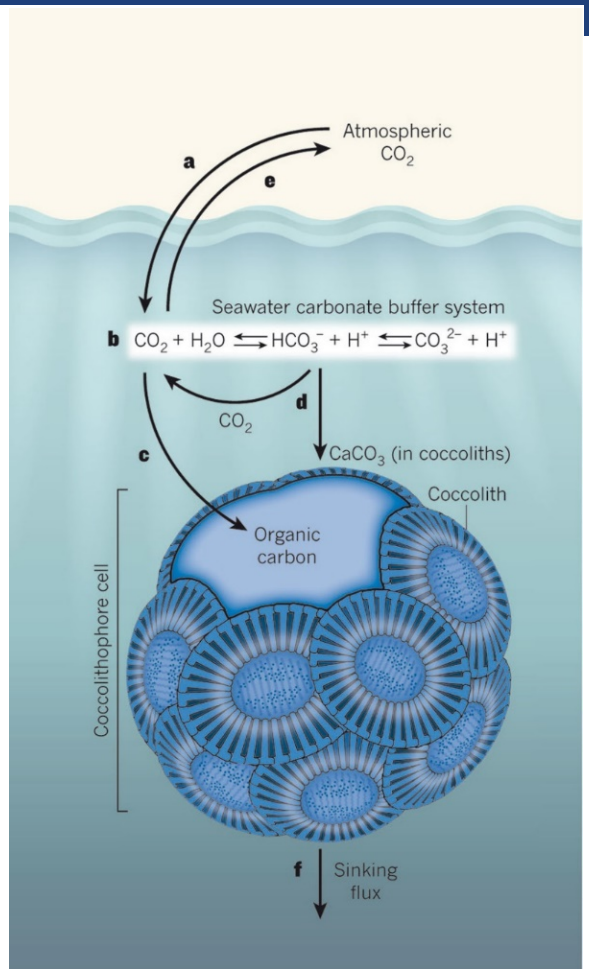

- This study assumes μ in two different ways:
  - μ ~ stratification of the upper water column ($\Delta^{18}O$ plankt. forams) as a nutrient limitation based on a global core-top calibration (Hernandez-Almeida et al. *in review*)
  - μ inversely modeled (Statistical model by Stoll et al. 2019) based on ice-core CO_2 and ε_p data from Site 1266 (assumed to be a modern analogue to Site 1088 during the Late Miocene)

Study Site ODP 1088

- Existing SST record shows a decrease of 5-6°C during the LMC
- Surface hydrology shows a strong "freshening", related to either changes in precipitation or north-ward movement of the polar front

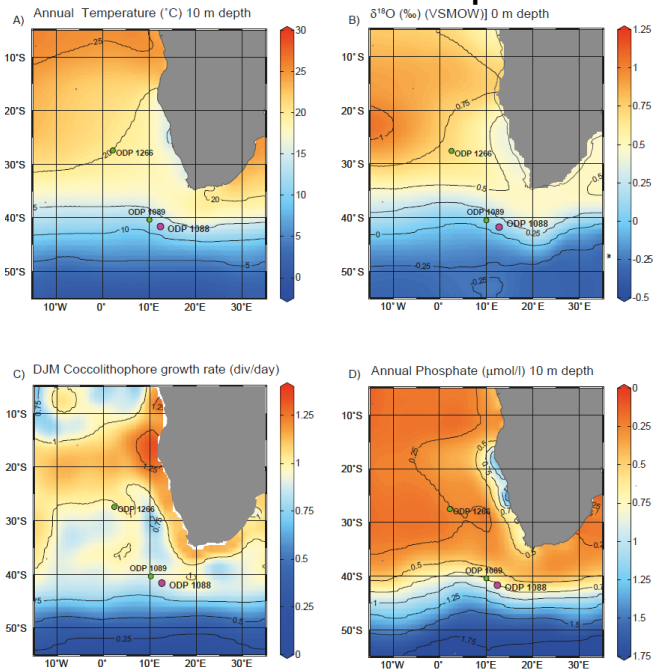

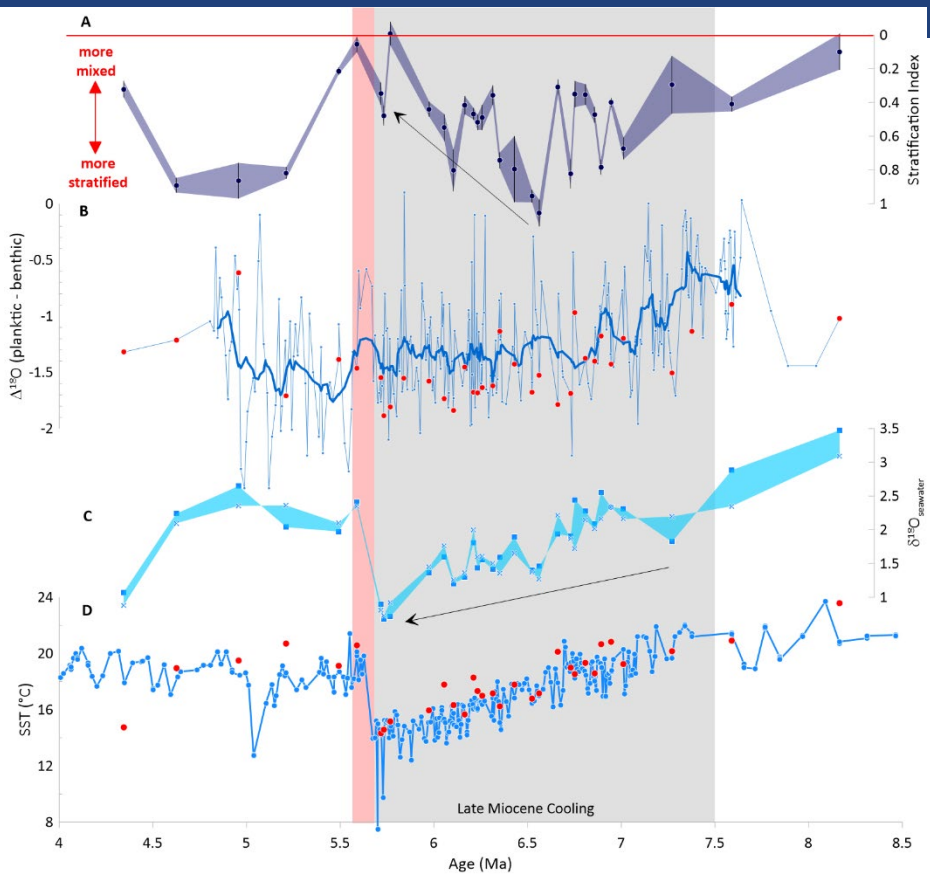

A) Stratification index showing how the upper water column structure changed over time. **B)** Gradient between planktic (*G. bulloides*) and benthic (*Cibicidoides spp.*) foraminifera (Billups et al., 2008), red dots show the data from this study. **C)** $\delta 18O_{seawater}$ calculated using the two intermediate-dwelling species *G. bulloides*, marked with a square, and *N. pachyderma*, marked with a cross. **D)** Alkenone based SST from Herbert et al. (2016) in blue. Red dots indicating new measurements from this study

DERDW
EARTH SCIENCES

Reconstructed CO_2 and additional datapoints

- Reconstruction based on a regression model for ε_p (Stoll et al. 2019)

$$\varepsilon_p \sim a * \ln CO_2 + b * \ln light + c * \mu + d * radius$$

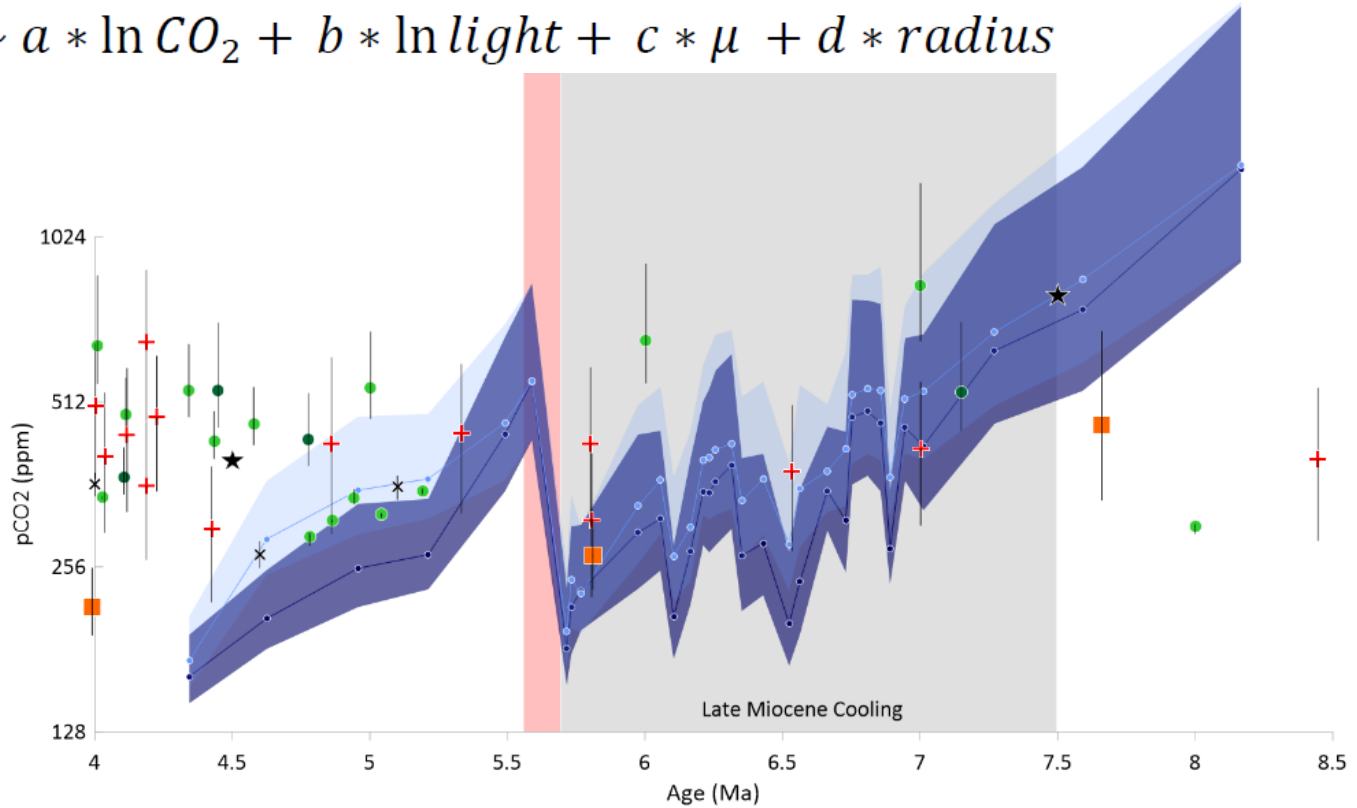

Light blue trend shows CO_2 values with growth rate μ inversely modeled, dark blue trend show CO_2 values with growth rate μ based on a global core top calibration. Additional proxy data: boron isotopes with red crosses (Sosdian et al., 2018), dark (ODP 925) and light (ODP 999) green dots from recalculated ε_p (Stoll et al., 2019), orange boxes (ODP 846) from diatom ε_p record (Mejía et al., 2017), black crosses from stomata index (Bai et al., 2015) and black stars from cGENIE modelling (Crichton et al., 2020)

Carbon Cycle

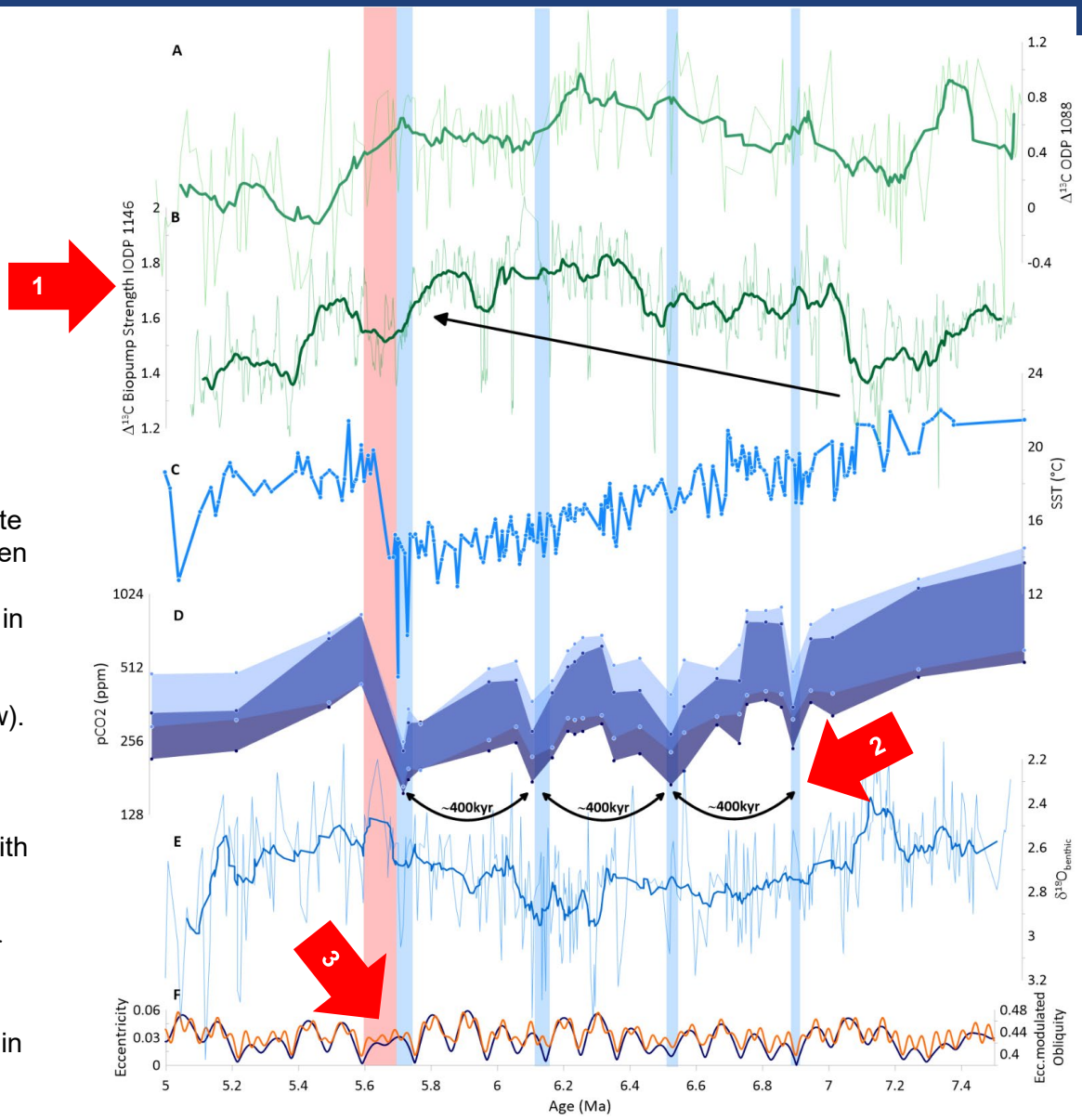

A) $\Delta^{13}C$ between planktic (*G. bulloides)* and benthic (*Cibicidoides spp*.) foraminifera at Site 1088 in the Southern Ocean. **B)** $\Delta^{13}C$ between planktic (*G. sacculifer)* and benthic (*Cibicidoides spp*.) foraminifera at Site 1146 in the South China Sea from Holbourn et al. (2018), showing an strengthening of the Pacific Ocean's biological pump (black arrow). **C)** Alkenone based SST from Herbert et al. (2016) at Site 1088. **D)** Most robust pCO2 trend over the LMC. Indicated are distinct 400kyr minimas, occurring simultaneously with 400kyr minimas in eccentricity. **E)** $\delta^{18}O_{benthic}$ from Site 1088 (Billups et al., 2008). **F)** Eccentricity and obliquity cycles after Laskar et al. (2004). Blue bars show times with 400kyr minimas in pCO_2 and eccentricity, simultaneously occurring as some maximas in $\delta^{18}O_{benthic}$

Summary

1. Indicators for the **biological pump** seem to show a **strengthening** during the Late Miocene Cooling. Records from the Southern Ocean (ODP 1088) and the South China Sea (IODP 1146) might explain the continuous long-term drawdown of atmospheric CO_2 described in this study.
2. Intriguingly, the continuous decrease in pCO_2 experiences distinct minimas **roughly every 400kyrs**, simultaneously occurring with 400kyr-minimas in eccentricity. These low pCO_2 values coincide with $\delta^{18}O_{benthic}$ maximas at Site 1088, potentially showing **periods of ice sheet expansion**. The reported pCO_2 values are low enough to pass the threshold and produce **ephemeral Northern Hemisphere glaciation** (DeConto et al. 2008), millions of years before its intensification.
3. The increase of pCO_2 and temperature at the end of the Late Miocene Cooling happens during an orbital constellation of relatively constant eccentricity. If and how this has an impact on the carbon cycle and the climate at the end of the Miocene is unclear. **Suggestions?**